PHYSICAL REVIEW B **79**, 155201 (2009)

Electron spin relaxation in paramagnetic Ga(Mn)As quantum wells

J. H. Jiang,[1] Y. Zhou,[1] T. Korn,[2] C. Schüller,[2] and M. W. Wu[1,*]

[1]*Hefei National Laboratory for Physical Sciences at Microscale and Department of Physics, University of Science and Technology of China, Hefei, Anhui, 230026, China*

[2]*Institut für Experimentelle und Angewandte Physik, Universität Regensburg, D-93040 Regensburg, Germany*

(Received 8 January 2009; revised manuscript received 25 February 2009; published 1 April 2009)

Electron spin relaxation in paramagnetic Ga(Mn)As quantum wells is studied via the fully microscopic kinetic spin Bloch equation approach where all the scatterings, such as the electron-impurity, electron-phonon, electron-electron Coulomb, electron-hole Coulomb, electron-hole exchange (the Bir-Aronov-Pikus mechanism) and the *s*-*d* exchange scatterings, are explicitly included. The Elliott-Yafet mechanism is also incorporated. From this approach, we study the spin relaxation in both *n*-type and *p*-type Ga(Mn)As quantum wells. For *n*-type Ga(Mn)As quantum wells, where most Mn ions take the interstitial positions, we find that the spin relaxation is always dominated by the D'yakonov-Perel' (DP) mechanism in the metallic region. Interestingly, the Mn concentration dependence of the spin relaxation time is nonmonotonic and exhibits a peak. This is due to the fact that the momentum scattering and the inhomogeneous broadening have different density dependences in the nondegenerate and degenerate regimes. For *p*-type Ga(Mn)As quantum wells, we find that the Mn concentration dependence of the spin relaxation time is also nonmonotonic and shows a peak. The cause of this behavior is that the *s*-*d* exchange scattering (or the Bir-Aronov-Pikus) mechanism dominates the spin relaxation in the high Mn concentration regime at low (or high) temperature, whereas the DP mechanism determines the spin relaxation in the low Mn concentration regime. The Elliott-Yafet mechanism also contributes to the spin relaxation at intermediate temperatures. The spin relaxation time due to the DP mechanism increases with increasing Mn concentration due to motional narrowing, whereas those due to the spin-flip mechanisms decrease with it, which thus leads to the formation of the peak. The temperature, photoexcitation density, and magnetic field dependences of the spin relaxation time in *p*-type Ga(Mn)As quantum wells are investigated systematically with the underlying physics revealed. Our results are consistent with the recent experimental findings.

DOI: 10.1103/PhysRevB.79.155201 PACS number(s): 72.25.Rb, 75.50.Pp, 71.10.−w, 71.70.Ej

I. INTRODUCTION

Semiconductors doped with magnetic impurities have intrigued much interest since the invention of ferromagnetic III-V semiconductors due to the possibility of integrating both the magnetic (spin) and charge degree of freedom on one chip.[1–7] Many new device conceptions and functionalities based on these materials are proposed, and the material properties together with the underlying physics are extensively studied.[4,8–16] Specifically, ferromagnetic $Ga_{1-x}Mn_xAs$ has been used as a highly efficient source to inject spin polarization into GaAs (Ref. 17) and magnetic tunneling junctions based on ferromagnetic $Ga_{1-x}Mn_xAs$ can achieve very high magnetoresistance.[18] Besides, the ability to detect the magnetic moment via Hall measurements[4,19] and to control it via gate-voltage[20] and laser radiation[21] opens the way for incorporating optoelectronics with magnetism. Magneto-optical measurements, which could characterize the spin splitting of carriers due to both the external magnetic field and the *s*-*d* or *p*-*d* exchange field, provide important information about the microscopic properties of the carriers, such as, the *g* factor, the *s*-*d* and *p*-*d* exchange coupling constants, as well as the electron spin relaxation time (SRT). Such measurements have recently been performed in dilutely doped paramagnetic Ga(Mn)As quantum wells.[22–25] Although many properties of Ga(Mn)As have been extensively studied, the electron spin relaxation has not yet been well understood even in dilutely doped paramagnetic phase. This is the aim of this investigation. We focus on (001) Ga(Mn)As quantum wells.

Electron spin relaxation in nonmagnetic GaAs has been extensively studied and three main spin relaxation mechanisms have been recognized for decades:[26] the D'yakonov-Perel' (DP) mechanism,[27] the Bir-Aronov-Pikus (BAP) mechanism[28] and the Elliott-Yafet (EY) mechanism.[29] Usually, the DP mechanism dominates the spin relaxation in *n*-type quantum wells.[10,30] The BAP mechanism was believed to be most important at low temperature in intrinsic and *p*-type quantum wells for a long time.[10,26] Recently, Zhou and Wu[31] showed that the BAP mechanism was exaggerated in the low-temperature regime in previous treatments based on the elastic-scattering approximation, where the Pauli blocking was not considered. It was then found that the BAP mechanism is less efficient than the DP mechanism in intrinsic quantum wells and *p*-type quantum wells with high photoexcitation density. A similar conclusion was also obtained in bulk GaAs very recently.[32] Previously, the EY mechanism was believed to dominate the spin relaxation in heavily doped samples at low temperature. However, it was shown to be unimportant in bulk GaAs by our recent investigation.[32] Whether this is still true in quantum-well systems remains unchecked. Moreover, in paramagnetic Ga(Mn)As quantum wells, things are more complicated: (i) all the three mechanisms could be important as the material is heavily doped with Mn and the hole density is generally very high.[22] (ii) An additional spin relaxation mechanism due to the exchange coupling of the electrons and the localized

Mn spins (the *s-d* exchange scattering mechanism) may also be important.[8] In this work, we will compare different spin relaxation mechanisms for various Mn concentrations, temperatures, photoexcitation densities, and magnetic fields.

In Ga(Mn)As, the Mn dopants can be either substitutional or interstitial; the substitutional Mn accepts one electron, whereas the interstitial Mn releases two. Direct doping in low-temperature molecular-beam epitaxy growth gives rise to more substitutional Mn ions than interstitial ones, which makes the Ga(Mn)As a *p*-type semiconductor.[8,9,22] Recently, it was found that in GaAs quantum wells near a Ga(Mn)As layer, the Mn dopants can diffuse into the GaAs quantum well, where the Mn ions mainly take the interstitial positions, making the quantum well *n* type.[23,24,33] The experimental results also show interesting features of the SRT.

We apply the fully microscopic kinetic spin Bloch equation (KSBE) approach[34,35] to investigate the spin relaxation in paramagnetic Ga(Mn)As quantum wells. The KSBE approach explicitly includes all relevant scatterings, such as, the electron-impurity, electron-phonon, electron-electron Coulomb, electron-hole Coulomb, electron-hole exchange (the BAP mechanism), and *s-d* exchange scatterings. Previously, the KSBE approach has been applied to study the spin dynamics in semiconductor and its nanostructures where good agreement with experiments have been achieved and many predictions have been confirmed by experiments.[30–32,34–49] In this work, we apply the KSBE approach to both *n*- and *p*-type paramagnetic Ga(Mn)As quantum wells to study the electron spin relaxation. We distinguish the dominant spin relaxation mechanisms in different regimes and our results are consistent with the recent experimental findings.

This paper is organized as follows: in Sec. II, we set up the model and establish the KSBEs. In Sec. III we present our results and discussions. We conclude in Sec. IV.

II. MODEL AND KSBES

We start our investigation from a paramagnetic [001] grown Ga(Mn)As quantum well of width a in the growth direction (the z axis). A moderate magnetic field $\mathbf{B}$ is applied along the x axis (the Voigt configuration). It is assumed that the well width is small enough so that only the lowest subband of electron and the lowest two subbands of heavy hole are relevant for the electron and hole densities in our investigation. The barrier layer is chosen to be $\mathrm{Al_{0.4}Ga_{0.6}As}$ where the barrier heights of electron and hole are 328 and 177 meV respectively.[50] The envelope functions of the relevant subbands are calculated via the finite-well-depth model.[30,31]

The KSBEs can be constructed via the nonequilibrium Green's function method[51] and read

$$\partial_t \hat{\rho}_{\mathbf{k}} = \partial_t \hat{\rho}_{\mathbf{k}}|_{\mathrm{coh}} + \partial_t \hat{\rho}_{\mathbf{k}}|_{\mathrm{scat}}, \tag{1}$$

with $\hat{\rho}_{\mathbf{k}}$ representing the single-particle density matrix whose diagonal and off-diagonal elements describe the electron distribution functions and the spin coherence respectively.[34] The coherent term is given by ($\hbar \equiv 1$ throughout this paper)

$$\partial_t \hat{\rho}_{\mathbf{k}}|_{\mathrm{coh}} = -i\left[(g_e \mu_{\mathrm{B}} \mathbf{B} + \mathbf{h}(\mathbf{k})) \cdot \frac{\hat{\boldsymbol{\sigma}}}{2} + \hat{H}_{\mathrm{sd}}^{\mathrm{mf}} + \hat{\Sigma}_{\mathrm{HF}}(\mathbf{k}), \hat{\rho}_{\mathbf{k}} \right], \tag{2}$$

in which [,] is the commutator. g_e is the electron g factor. $\mathbf{h}(\mathbf{k})$ represents the spin-orbit coupling (SOC), which is composed of the Dresselhaus[52] and Rashba[53] terms. In symmetric GaAs quantum well with small well width, the Dresselhaus term is dominant[54] and

$$\mathbf{h}(\mathbf{k}) = 2\gamma_{\mathrm{D}}(k_x(k_y^2 - \langle k_z^2 \rangle), k_y(\langle k_z^2 \rangle - k_x^2), 0). \tag{3}$$

Here $\langle k_z^2 \rangle$ represents the average of the operator $-(\partial/\partial z)^2$ over the state of the lowest electron subband and $\gamma_{\mathrm{D}} = 8.6\ \mathrm{eV\ Å^3}$ is the Dresselhaus SOC coefficient.[30] The mean-field contribution of the *s-d* exchange interaction is given by

$$\hat{H}_{\mathrm{sd}}^{\mathrm{mf}} = -N_{\mathrm{Mn}} \alpha \langle \mathbf{S} \rangle \frac{\hat{\boldsymbol{\sigma}}}{2}, \tag{4}$$

where $\langle \mathbf{S} \rangle$ is the average spin polarization of Mn ions and α is the *s-d* exchange coupling constant. For simplicity, we assume that the Mn ions are uniformly distributed within and around the Ga(Mn)As quantum well with a bulk density N_{Mn}. $\hat{\Sigma}_{\mathrm{HF}}(\mathbf{k}) = -\Sigma_{\mathbf{q},q_z} V_{\mathbf{q},q_z} |I(iq_z)|^2 \hat{\rho}_{\mathbf{k}-\mathbf{q}}$ is the Coulomb Hartree-Fock (HF) term, where $I(iq_z) = \int dz |\xi_e(z)|^2 e^{iq_z z}$ is the form factor with $\xi_e(z)$ standing for the envelope function of the lowest electron subband.[35] $V_{\mathbf{q},q_z}$ is the screened Coulomb potential. In this work, we take into account the screening from both electrons and holes within the random-phase approximation.[31]

The scattering term $\partial_t \hat{\rho}_{\mathbf{k}}|_{\mathrm{scat}}$ consists of the electron-impurity, electron-electron Coulomb, electron-phonon, electron-hole Coulomb, electron-hole exchange and *s-d* exchange scatterings. The expressions of all these terms except the *s-d* exchange scattering can be found in Ref. 31. However, the expression of the electron-impurity scattering term with the EY mechanism included has not been given in that paper, which we will present later in this paper. The *s-d* exchange scattering term is given by

$$\begin{aligned} \partial_t \hat{\rho}_{\mathbf{k}}|_{\mathrm{sd}}^{\mathrm{scat}} = {} & -\pi N_{\mathrm{Mn}} \alpha^2 I_s \sum_{\eta_1 \eta_2 \mathbf{k}'} G_{\mathrm{Mn}}(-\eta_1 - \eta_2) \delta(\varepsilon_{\mathbf{k}} - \varepsilon_{\mathbf{k}'}) \\ & \times [\hat{s}^{\eta_1} \hat{\rho}_{\mathbf{k}'}^{>} \hat{s}^{\eta_2} \hat{\rho}_{\mathbf{k}}^{<} - \hat{s}^{\eta_2} \hat{\rho}_{\mathbf{k}'}^{<} \hat{s}^{\eta_1} \hat{\rho}_{\mathbf{k}}^{>} + \mathrm{H.c.}]. \end{aligned} \tag{5}$$

Here $\hat{\rho}_{\mathbf{k}}^{>} = \hat{1} - \hat{\rho}_{\mathbf{k}}$, $\hat{\rho}_{\mathbf{k}}^{<} = \hat{\rho}_{\mathbf{k}}$, $G_{\mathrm{Mn}}(\eta_1 \eta_2) = \frac{1}{4}\mathrm{Tr}(\hat{S}^{\eta_1} \hat{S}^{\eta_2} \hat{\rho}_{\mathrm{Mn}})$, and $I_s = \int dz |\xi_e(z)|^4$. $\hat{S}^{\eta}$ and $\hat{s}^{\eta}(\eta = 0, \pm 1)$ are the spin ladder operators with $\hat{S}^0 = \hat{S}_z$, $\hat{S}^{\pm} = \hat{S}_x \pm i\hat{S}_y$, $\hat{s}^0 = 2\hat{s}_z$, and $\hat{s}^{\pm} = \hat{s}_x \pm i\hat{s}_y$. $\hat{\rho}_{\mathrm{Mn}}$ is the Mn spin density matrix. $\varepsilon_{\mathbf{k}} = k^2/2m^*$ is the electron kinetic energy with m^* denoting the effective mass. The equation of motion for Mn spin density matrix consists of three parts $\partial_t \hat{\rho}_{\mathrm{Mn}} = \partial_t \hat{\rho}_{\mathrm{Mn}}|_{\mathrm{coh}} + \partial_t \hat{\rho}_{\mathrm{Mn}}|_{\mathrm{scat}} + \partial_t \hat{\rho}_{\mathrm{Mn}}|_{\mathrm{rel}}$. The first part describes the coherent precession around the external magnetic field and the *s-d* exchange mean field, $\partial_t \hat{\rho}_{\mathrm{Mn}}|_{\mathrm{coh}} = -i[g_{\mathrm{Mn}} \mu_{\mathrm{B}} \mathbf{B} \cdot \hat{\mathbf{S}} - \alpha \Sigma_{\mathbf{k}} \mathrm{Tr}(\frac{\hat{\boldsymbol{\sigma}}}{2} \hat{\rho}_{\mathbf{k}}) \cdot \hat{\mathbf{S}}, \hat{\rho}_{\mathrm{Mn}}]$. The second part represents the *s-d* exchange scattering with electrons $\partial_t \hat{\rho}_{\mathrm{Mn}}|_{\mathrm{scat}} = -\frac{\pi \alpha^2}{4} \Sigma_{\eta_1 \eta_2 \mathbf{k}} \delta(\varepsilon_{\mathbf{k}} - \varepsilon_{\mathbf{k}'}) \mathrm{Tr}(\hat{s}^{-\eta_2} \hat{\rho}_{\mathbf{k}'}^{<} \hat{s}^{-\eta_1} \hat{\rho}_{\mathbf{k}}^{>}) [(\hat{S}^{\eta_1} \hat{S}^{\eta_2} \hat{\rho}_{\mathrm{Mn}}$

$-\hat{S}^{\eta_1}\hat{\rho}_{\rm Mn}\hat{S}^{\eta_2})+{\rm H.c.}]$. The third term characterizes the Mn spin relaxation due to other mechanisms, such as, *p*-*d* exchange interaction with holes or Mn spin-lattice interactions, with a relaxation time approximation, $\partial_t\hat{\rho}_{\rm Mn}|_{\rm rel}=-(\hat{\rho}_{\rm Mn}-\hat{\rho}^0_{\rm Mn})/\tau_{\rm Mn}$. Here $\hat{\rho}^0_{\rm Mn}$ represents the equilibrium Mn spin density matrix. $\tau_{\rm Mn}$ is the Mn spin relaxation time, which is typically 0.1–10 ns.[55] In our calculation we take $\tau_{\rm Mn}=1$ ns. At $t=0$, the Mn spin density matrix is chosen to be the equilibrium one $\hat{\rho}^0_{\rm Mn}$. The Mn spins can be dynamically polarized via the *s*-*d* exchange interaction, and feedback to the electron spin dynamics. However, we find that this process affects the electron spin dynamics little. Hence, the choice of $\tau_{\rm Mn}$ does not affect our discussions on electron spin dynamics.

The *s*-*d* exchange scattering $\tau_{\rm sd}$ can be obtained analytically. In the absence of an external magnetic field, the spin polarization of the electron system is always along the *z* direction. As the *s*-*d* exchange interaction conserves the spin polarization of the total system, the spin polarization of Mn ions (which is assumed to be zero initially) can only be along the *z* direction. By keeping only the diagonal term of $\hat{\rho}_{\rm Mn}$, from the Fermi Golden rule, the spin relaxation time due to the *s*-*d* exchange scattering can be obtained directly,

$$\tau_{\rm sd}=\left\{\frac{1}{2}N_{\rm Mn}I_s\alpha^2m^*[S(S+1)-\langle S_z^2\rangle]\right\}^{-1}=\frac{12}{35N_{\rm Mn}\alpha^2m^*I_s}, \tag{6}$$

where $S=5/2$ is the spin of the Mn ion. It is evident that $\tau_{\rm sd}$ is independent of temperature and electron density, but is inverse proportional to Mn concentration $N_{\rm Mn}$, the square of the *s*-*d* exchange coupling α^2 and $I_s=\int dz|\xi_e(z)|^4$. I_s is determined by the confinement of the quantum well. For an infinite depth well $I_s=\frac{3}{2a}$, thus $\tau_{\rm sd}$ is proportional to the well width a.

After incorporating the EY mechanism, besides the ordinary spin-conserving term, there are spin-flip terms. For electron-impurity scattering these additional terms are

$$\begin{aligned}\partial_t\hat{\rho}_{\mathbf{k}}|^{\rm EY}_{\rm ei}=&-\pi n_i\sum_{\mathbf{k}'}\delta(\varepsilon_{\mathbf{k}}-\varepsilon_{\mathbf{k}'})[U^{(1)}_{\mathbf{k}-\mathbf{k}'}(\hat{\Lambda}^{(1)}_{\mathbf{k},\mathbf{k}'}\hat{\rho}^{>}_{\mathbf{k}'}\hat{\Lambda}^{(1)}_{\mathbf{k}',\mathbf{k}}\\&\times\hat{\rho}^{<}_{\mathbf{k}}-\hat{\Lambda}^{(1)}_{\mathbf{k},\mathbf{k}'}\hat{\rho}^{<}_{\mathbf{k}'}\hat{\Lambda}^{(1)}_{\mathbf{k}',\mathbf{k}}\hat{\rho}^{>}_{\mathbf{k}})+U^{(2)}_{\mathbf{k}-\mathbf{k}'}(\hat{\Lambda}^{(2)}_{\mathbf{k},\mathbf{k}'}\hat{\rho}^{>}_{\mathbf{k}'}\\&\times\hat{\Lambda}^{(2)}_{\mathbf{k}',\mathbf{k}}\hat{\rho}^{<}_{\mathbf{k}}-\hat{\Lambda}^{(2)}_{\mathbf{k},\mathbf{k}'}\hat{\rho}^{<}_{\mathbf{k}'}\hat{\Lambda}^{(2)}_{\mathbf{k}',\mathbf{k}}\hat{\rho}^{>}_{\mathbf{k}})+{\rm H.c.}],\end{aligned} \tag{7}$$

where $n_i=N^{\rm S}_{\rm Mn}+4N^{\rm I}_{\rm Mn}+n_{i0}$ with $N^{\rm S}_{\rm Mn}$, $N^{\rm I}_{\rm Mn}$, and n_{i0} being the densities of substitutional Mn, interstitial Mn and nonmagnetic impurities, respectively, due to different charges. $U^{(1)}_{\mathbf{k}-\mathbf{k}'}=\frac{\lambda_c^2}{4}\Sigma_{q_z}V^2_{\mathbf{k}-\mathbf{k}',q_z}|I(iq_z)|^2q_z^2$ and $U^{(2)}_{\mathbf{k}-\mathbf{k}'}=-\lambda_c^2\Sigma_{q_z}V^2_{\mathbf{k}-\mathbf{k}',q_z}|I(iq_z)|^2$. Here $\lambda_c=\frac{\eta(1-\eta/2)}{3m_cE_g(1-\eta/3)}$ with $\eta=\frac{\Delta_{\rm SO}}{\Delta_{\rm SO}+E_g}$. E_g and $\Delta_{\rm SO}$ are the band gap and the spin-orbit splitting of the valence band, respectively.[26] The spin-flip matrices are given by $\hat{\Lambda}^{(1)}_{\mathbf{k}',\mathbf{k}}=[(\mathbf{k}+\mathbf{k}',0)\times\hat{\boldsymbol{\sigma}}]_z$ and $\hat{\Lambda}^{(2)}_{\mathbf{k},\mathbf{k}'}=[(\mathbf{k},0)\times(\mathbf{k}',0)]\cdot\hat{\boldsymbol{\sigma}}$. It is noted that $\hat{\Lambda}^{(1)}_{\mathbf{k}',\mathbf{k}}$ and $\hat{\Lambda}^{(2)}_{\mathbf{k}',\mathbf{k}}$ contribute to the out-of-plane and in-plane spin relaxations, respectively. They are generally different and therefore the spin relaxation due to the EY mechanism in quantum wells is anisotropic. The EY mechanism can be incorporated into other scatterings similarly.[32] However, we find that the EY mechanism can be important only when the impurity density is high, where the electron-impurity scattering is most important. Therefore, for simplicity, we include only the EY spin-flip processes associated with the electron-impurity scattering.

TABLE I. Material parameters used in the calculation.

κ_0	12.9	κ_∞	10.8
D	5.31×10^3 kg/m^3	e_{14}	1.41×10^9 V/m
v_{st}	2.48×10^3 m/s	v_{sl}	5.29×10^3 m/s
Ξ	8.5 eV	$\omega_{\rm LO}$	35.4 meV
$\Delta_{\rm SO}$	0.341 eV	E_g	1.55 eV
ΔE_{LT}	0.08 meV	a_0	146.1 Å
g_e	−0.44	m^*	$0.067m_0$
$g_{\rm Mn}$	2	S	5/2

III. RESULTS AND DISCUSSIONS

By solving the KSBEs numerically, we obtain the temporal evolution of the single-particle density matrix $\hat{\rho}_{\mathbf{k}}$ and then the spin polarization along the *z* axis, i.e., s_z. From the decay of s_z, the SRT is extracted. The initial spin polarization is chosen to be $P=4\%$. The well width $a=10$ nm. The external magnetic field $\mathbf{B}$ is zero unless otherwise specified. We use x to denote the Mn density, where $N_{\rm Mn}=xN_0$ with $N_0=\Omega^{-1}=2.22\times10^{22}$ cm^{-3} (Ω is the volume of the unit cell in GaAs). The other material parameters used are listed in Table I.[56–58]

The value of the *s*-*d* exchange coupling in III(Mn)V materials is still in dispute. In bulk Ga(Mn)As, first-principles calculation gives the value $N_0\alpha\approx0.25$ eV.[59] However, the experimental measurements in Ref. 22 show that $N_0\alpha$ is in the range of $[-0.21,-0.07]$ eV varying with quantum well width. In this paper, we choose $N_0\alpha=-0.15$ eV unless otherwise specified.

A. Spin relaxation in *n*-type Ga(Mn)As quantum wells

In this subsection, we study the electron spin relaxation in *n*-type Ga(Mn)As quantum wells, where the Mn dopants mainly take interstitial positions. For simplicity, we neglect the substitutional Mn's and assume that electrons from Mn donors are all free electrons. We will discuss the situations that the quantum wells are either undoped or *n*-doped before Mn-doping.

For quantum wells which are undoped before Mn-doping, $N_e=N_e^{\rm Mn}+N_{\rm ex}$ where $N_e^{\rm Mn}$ is the density of electrons from Mn donors and $N_{\rm ex}$ is the photoexcitation density. We choose $N_{\rm ex}=10^{10}$ cm^{-2} which is usually smaller than $N_e^{\rm Mn}$. The SRTs due to various mechanisms are plotted as function of x in Fig. 1(a). $N_0\alpha$ is chosen to be −0.25 eV, which is smaller (i.e., the *s*-*d* exchange interaction is stronger) than the value measured by experiments.[22] However, even for such a strong exchange coupling, the spin relaxation due to the *s*-*d* exchange scattering mechanism is *still* much weaker than that due to the DP mechanism. It is further seen from Fig. 1(a)

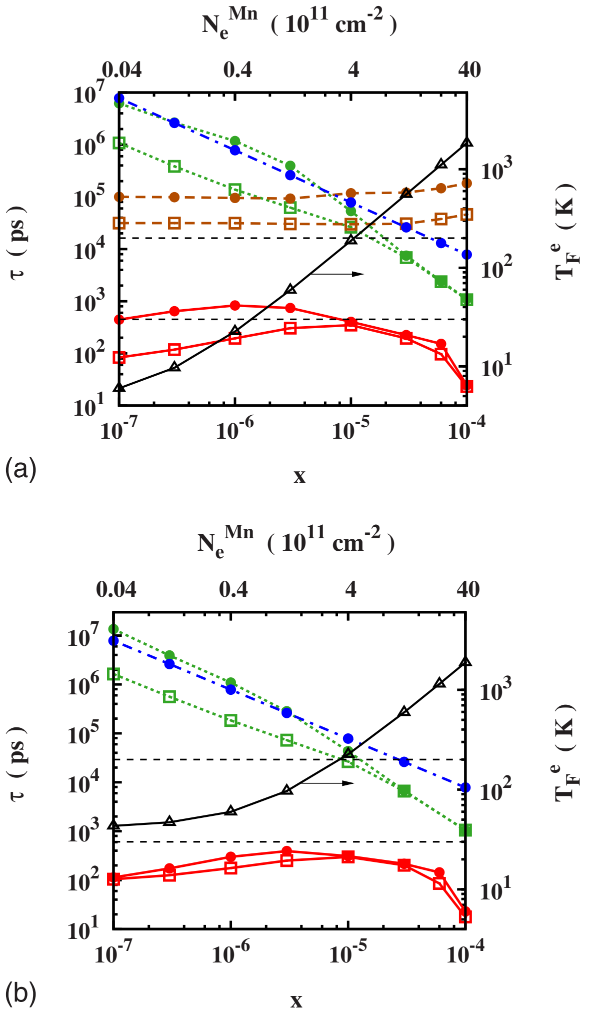

FIG. 1. (Color online) SRT τ due to various mechanisms in n-type Ga(Mn)As quantum wells which are (a) undoped or (b) n-doped before Mn-doping as function of Mn concentration x at 30 K (●) and 200 K (□). Red solid curves: the SRT due to the DP mechanism τ_{DP}; green dotted curves: the SRT due to the EY mechanism τ_{EY}; brown dashed curves: the SRT due to the BAP mechanism τ_{BAP}; blue chain curve: the SRT due to the s-d exchange scattering mechanism τ_{sd}. The Fermi temperature of electrons T_F^e is plotted as black curve with △ (the scale of T_F^e is on the right-hand side of the frame) and $T_F^e = T$ for both $T=30$ and 200 K cases are plotted as black dashed curves. We also plot the scale of the electron density from Mn donors N_e^{Mn} on the top of the frame.

that the BAP and EY mechanisms are also unimportant. Therefore, the SRT is determined by the DP mechanism. Interestingly, the SRT due to the DP mechanism τ_{DP} first increases then decreases with increasing x. The τ-x curve thus has a peak. The underlying physics is that the SRT has different x (density) dependence in the nondegenerate and degenerate regimes. Similar behavior has been found in bulk nonmagnetic III-V semiconductors in Ref. 32 very recently. Let us first recall the widely used expression, $\tau_{\mathrm{DP}} = 1/[\langle|\mathbf{h}(\mathbf{k})|^2\rangle\tau_p]$ ($\langle\cdots\rangle$ denotes the ensemble average), which is derived within the elastic-scattering approximation and is only correct qualitatively.[32] The expression contains two key factors of the DP spin relaxation: (i) the inhomogeneous broadening from the $\mathbf{k}$-dependent spin-orbit field $\sim\langle|\mathbf{h}(\mathbf{k})|^2\rangle$; (ii) the momentum scattering time τ_p. The SRT due to the DP mechanism increases with increasing momentum scattering but decreases with increasing inhomogeneous broadening. It should be mentioned that for this system, $N_e \approx n_i/2 = 2xN_0$ (Note that the charge number Z of the Mn ion is included in n_i as Z^2. For interstitial Mn, which acts as a double donor, $Z=2$.) In the small x (low density) regime, the electron system is in the nondegenerate regime, and the distribution is close to the Boltzmann distribution. Therefore, the inhomogeneous broadening of the $\mathbf{k}$ dependent spin-orbit field $\sim\langle|\mathbf{h}(\mathbf{k})|^2\rangle$ changes little with electron density N_e (hence x). On the other hand, in the nondegenerate regime the electron-electron scattering increases with increasing electron density[60,61] (thus x). Moreover, the electron-impurity scattering also increases with increasing x as the impurity density increases. Therefore, τ_{DP} increases with increasing x (motional narrowing). In large x (high density) regime, the electron system is in the degenerate regime, the inhomogeneous broadening changes as $k_F^2 \propto N_e \propto x(k_F^6 \propto N_e^3 \propto x^3)$ if the linear (cubic) term dominates the SOC. On the other hand, the electron-electron scattering decreases with increasing electron density (thus x) in the degenerate regime.[60,61] Besides, the electron-impurity scattering increases slower than $N_i \propto x$ because the scattering cross section decreases as the electron (Fermi) energy increases. Thus for both the linear- and cubic-term dominant cases, τ_{DP} decreases with increasing x in the large x regime. Consequently, τ_{DP} first increases then decreases with increasing x and a peak is formed in the crossover regime where $T \sim T_F^e$ (T_F^e is the electron Fermi temperature). It is seen from Fig. 1(a) that for both $T=30$ and 200 K cases, the peaks indeed appear at $T \sim T_F^e$. It should be pointed out that the situation here is different from that in Ref. 42, where the density dependence of the SRT also has a peak in intrinsic quantum wells at room temperature. In that case, the impurity density is rather low and the relevant momentum scatterings are the carrier-carrier Coulomb and electron-phonon scatterings. In the situation here, the impurity density is extremely high ($n_i = 2N_e$) and the relevant momentum scattering is the electron-impurity scattering.

We now turn to the situation that the quantum wells are n doped before Mn-doping. In this case, $N_e = N_e^i + N_e^{\mathrm{Mn}} + N_{\mathrm{ex}}$, where N_e^i denotes the density of the electrons from other dopants which is chosen to be 10^{11} cm^{-2}. We assume that the other dopants are far away from the quantum wells, so that they contribute little to the electron-impurity scattering, corresponding to the genuine case of modulation doping. However, the Mn ions are doped in the quantum wells.[23,24] The photoexcitation density is $N_{\mathrm{ex}} = 10^{10}$ cm^{-2}. The results are plotted in Fig. 1(b). As the density of the photoexcited holes is much smaller than the electron density, the BAP mechanism is obviously negligible and thus not plotted in the figure. From the figure, it is noted that the EY and s-d exchange scattering mechanisms are also insignificant. Consequently, the spin relaxation is still dominated by the DP mechanism. Similar to that in Fig. 1(a), the SRT due to the DP mechanism τ_{DP} first increases then decreases with increasing x. For the case of $T=200$ K, the peak of the SRT is still around $T = T_F^e$. However, for the case of $T=30$ K, the peak moves to a larger x value compared to that in Fig. 1(a).

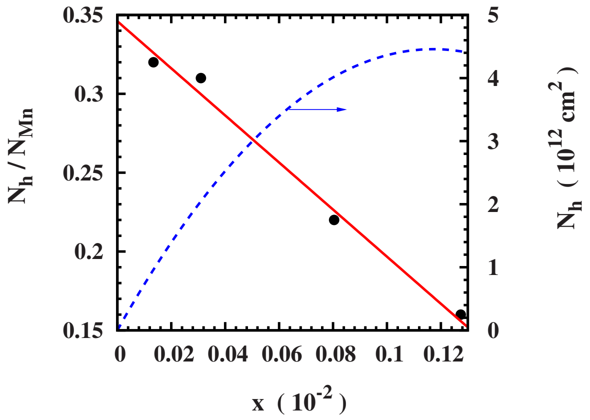

FIG. 2. (Color online) Ratio of the hole density to the Mn density N_h/N_{Mn} vs the Mn concentration x in p-type Ga(Mn)As quantum wells. The black dots represent the experimental data. The red solid curve is the fitted one. The hole density N_h is also plotted (the blue dashed curve). Note that the scale of N_h is on the right-hand side of the frame.

This can be understood by noting that the electrons have two sources: the Mn donors and other dopants. For the case of $T=200$ K, the crossover of the nondegenerate and degenerate regimes takes place around $T\sim T_{\mathrm{F}}^{e}$, where the corresponding x is 10^{-5}. At such x, electrons are mainly from the Mn ions rather than from other dopants. Thus the situation is the same as that in Fig. 1(a) and the peak appears at $T\sim T_{\mathrm{F}}^{e}$. However, in the case of $T=30$ K, for all x in the figure, T_{F}^{e} is larger than T and the situation is hence different. The τ-x behavior in this case can be understood as follows: for $x<10^{-6}$, electrons are mainly from the other dopants and N_e changes slowly with x, thus the inhomogeneous broadening varies slowly with x. On the other hand, the electron-impurity scattering increases as the impurity density increases $n_i\approx 4xN_0$. At low temperature ($T<T_{\mathrm{F}}^{e}$), the electron-impurity scattering can be important even when $n_i<N_e$.[30,32] Therefore, the momentum scattering increases with x significantly. Consequently, τ_{DP} increases with increasing x. For $x>10^{-5}$, electrons mainly come from the Mn donors. The scenario becomes the same as that in the case of Fig. 1(a) and the SRT decreases with increasing x as T_{F}^{e} is much larger than T. Consequently, the peak is formed in the range $10^{-6}<x<10^{-5}$ at $x=3\times 10^{-6}$, which is larger than that in the case of $T=30$ K in Fig. 1(a).

It should be mentioned that our results are consistent with the latest experimental finding that in the low Mn concentration regime the SRT increases with increasing x.[23,24]

B. Electron spin relaxation in *p*-type Ga(Mn)As quantum wells

In this section, we discuss the electron spin relaxation in p-type Ga(Mn)As quantum wells. Both substitutional and interstitial Mn ions exist in the system. Each substitutional Mn donates one hole, whereas each interstitial Mn compensates two holes. For simplicity, we assume that all the holes are free. The ratio of the hole density N_h to the Mn density N_{Mn} is obtained by fitting the experimental data in Ref. 22, as shown in Fig. 2. From these densities, according to charge neutrality, the densities of substitutional Mn $N_{\mathrm{Mn}}^{\mathrm{S}}$ and interstitial Mn $N_{\mathrm{Mn}}^{\mathrm{I}}$ are determined. The photoexcitation density is chosen to be $N_{\mathrm{ex}}=5\times 10^{10}$ cm^{-2} unless otherwise specified.

1. Mn concentration dependence of the SRT

We first study the Mn concentration dependence of the SRT. In Fig. 3, we plot the SRTs due to various mechanisms and the total SRT as function of the Mn concentration x at $T=5$, 50, and 200 K. It is noted that the total SRT first increases and then decreases with increasing x and there is a peak at $x\sim 3\times 10^{-5}$. Remarkably, the spin relaxation at large x is not dominated by the DP mechanism, but by the s-d exchange scattering (or the BAP) mechanism at low (or high) temperature. At medium temperature, the EY mechanism also contributes for large x. The SRT due to the DP mechanism increases with increasing x, whereas those due to the s-d exchange, EY, and BAP mechanisms decrease with increasing x. Consequently a peak is formed. It should be pointed out that the underlying physics here is different from that in the case of n-type Ga(Mn)As quantum well where the peak is solely due to the electron density dependence of the DP spin relaxation. It should be mentioned that the peak position is $x\sim 10^{-4}$, which is consistent with that observed in Ref. 22.

Let us now turn to the x dependence of the SRT due to various mechanisms. The increase in τ_{DP} with increasing x is due to the increase in the electron-impurity and electron-hole scatterings (motional narrowing). For the EY mechanism, the SRT decreases as the spin-flip scattering increases with increasing impurity density [see Eq. (7)]. The s-d exchange scattering increases with increasing x as the Mn density increases [see Eq. (5)]. The x dependence of the BAP spin relaxation is more complicated. To facilitate the understanding, we plot τ_{BAP} from the full calculation and that from the calculations without the Pauli blocking of electrons (holes) in Fig. 4. It is seen that for $x<10^{-6}$, τ_{BAP} changes little with x. This is due to the fact that the holes from Mn dopants are much fewer than those from photoexcitation, and hence N_h changes little with x. So does τ_{BAP}. For larger x, τ_{BAP} first decreases then increases a little and finally saturates with increasing x at $T=5$ K. It is noted that without the Pauli blocking of holes, τ_{BAP} decreases with increasing x rapidly, which indicates that the slowdown of the decrease and the saturation of τ_{BAP} are due to the Pauli blocking of holes. It is further shown that the Pauli blocking of electrons is also important as $T_{\mathrm{F}}^{e}=20$ K is larger than $T=5$ K. For the case of $T=200$ K, the effect of the Pauli blocking of electrons is negligible as $T\gg T_{\mathrm{F}}^{e}$. The Pauli blocking of holes becomes visible only for $x>10^{-4}$, where the hole Fermi temperature becomes larger than $T=200$ K.

From Eq. (5), one can see that the spin relaxation due to the s-d exchange scattering is independent of temperature. However, the spin relaxation due to the BAP mechanism increases with increasing temperature because the Pauli blocking of electrons and holes decreases with increasing temperature. Moreover, the matrix element of the BAP mechanism increases with the center-of-mass momentum of the interacting electron-hole pair, of which the ensemble average hence increases with increasing temperature.[31] The

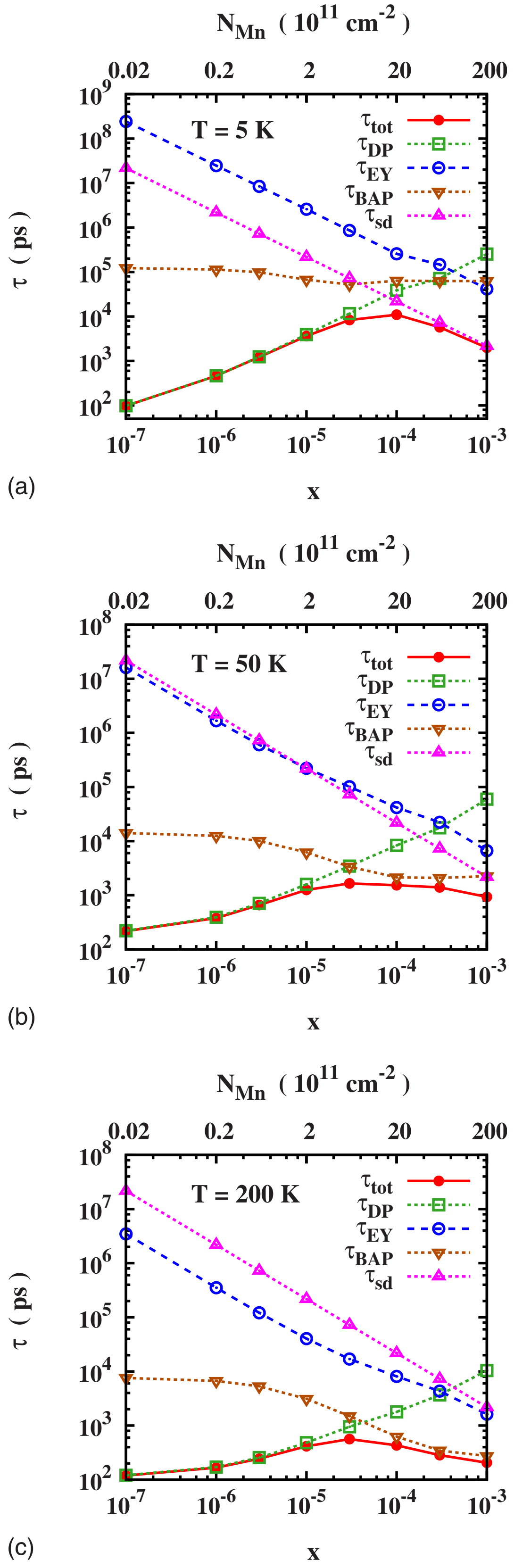

FIG. 3. (Color online) SRT τ due to various mechanisms and the total SRT in p-type Ga(Mn)As against the Mn concentration x at (a) $T=5$, (b) 50, and (c) 200 K. We also plot the scale of N_{Mn} on the top of the frame.

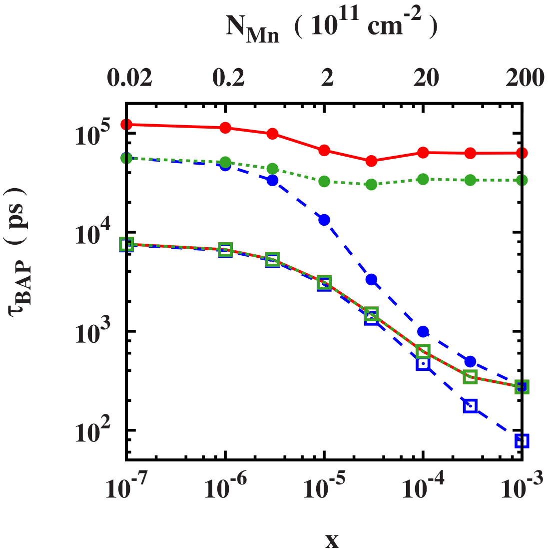

FIG. 4. (Color online) SRT due to the BAP mechanism τ_{BAP} as function of the Mn concentration at $T=5$ (●) and 200 K (□). Red solid curves: τ_{BAP} from the full calculation; green dotted curves: τ_{BAP} from the calculation without the Pauli blocking of electrons; blue dashed curves: τ_{BAP} from the calculation without the Pauli blocking of holes.

spin relaxation due to the EY mechanism increases with increasing temperature too, as the spin-flip matrices $[\hat{\Lambda}^{(1)}_{\mathbf{k}',\mathbf{k}}$ and $\hat{\Lambda}^{(2)}_{\mathbf{k}',\mathbf{k}}]$ in Eq. (7) increase with increasing k. Consequently, the BAP and EY mechanisms eventually become more efficient than the s-d exchange scattering mechanism at high temperature.

The appearance of the peak in the τ-x curve has been observed in a recent experiment at 5 K.[22] However, the SRTs we obtain are much larger than the experimental value under the same conditions. The deviation may come from pretermission of localized holes. At such low temperature (5 K), the localization of holes is not negligible.[26,62] The localized holes act as exchange interaction centers located randomly in the sample, which thus lead to spin relaxation similar to the s-d exchange scattering mechanism. As there is no Pauli blocking of the localized holes, the spin relaxation can be very efficient.[26] It should be mentioned that, however, recent studies have also shown that there is some compensation of the s-d exchange interaction and the electron-hole exchange interaction as holes are always localized on the Mn acceptors.[63,64] This leads to a longer spin relaxation time[63] and smaller measured (by magneto-optical techniques) s-d exchange coupling constant.[64] However, for the high-temperature case, the localization is marginal and our consideration is close to the genuine case. The predicted τ-x dependence should be tested experimentally.

2. Temperature dependence of the SRT

We now discuss the temperature dependence of the SRT. In Fig. 5, we plot the SRT as function of Mn concentration x for different temperatures. It is seen that for each case the τ-x curve shows a peak. It is further noted that the temperature

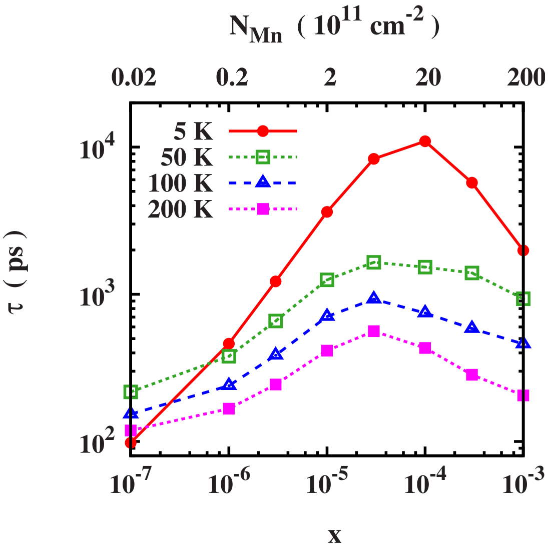

FIG. 5. (Color online) SRT τ as function of Mn concentration x at different temperatures.

dependences of the SRT are different for small (e.g., $x=10^{-7}$) and large x (e.g., $x=10^{-3}$). To make it more pronounced, we further plot the temperature dependence of the SRT for $x=10^{-7}$, 3×10^{-5}, and 10^{-3} in Fig. 6. For $x=10^{-7}$, the SRT first increases then decreases with increasing temperature and there is a peak around 20 K. It is understood that for such a small x, the electrons and holes are mainly from the photoexcitation. For such system, the electron-electron and electron-hole Coulomb scatterings are most important. It is shown in Ref. 30 that the nonmonotonic temperature dependence of the electron-electron Coulomb scattering leads to a peak in the τ-T curve. In the situation here, the electron-hole Coulomb scattering also contributes to the formation of the peak. For the case of $x=3\times10^{-5}$, all spin relaxation mechanisms are relevant and the most important momentum scattering is the electron-impurity scattering. In this case the SRT due to the DP mechanism decreases with increasing temperature monotonically as the increase in the inhomogeneous broadening dominates.[30] Moreover, the SRTs due to the EY and BAP mechanisms also decrease with increasing temperature. Consequently, the total SRT decreases with increasing temperature monotonically. For the case of large $x(x=10^{-3})$, the spin relaxation is dominated by the *s*-*d* exchange scattering (or the BAP) mechanism at low (or high) temperature. As the *s*-*d* exchange scattering mechanism is independent of the temperature, the temperature dependence is rather weak in the low-temperature regime. As the temperature increases, the EY and BAP mechanisms become more and more important, which leads to a fast decrease in the SRT with temperature.

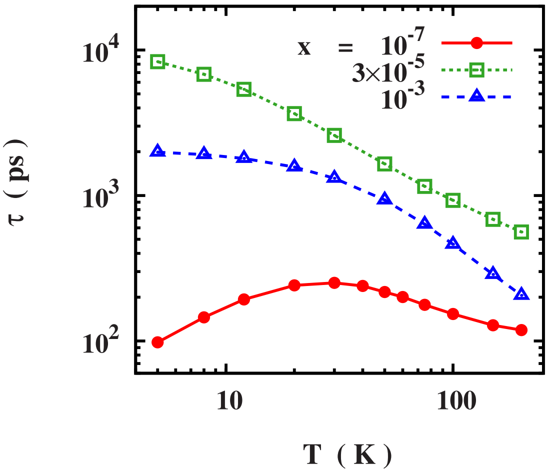

FIG. 6. (Color online) SRT τ as function of temperature T for different Mn concentrations.

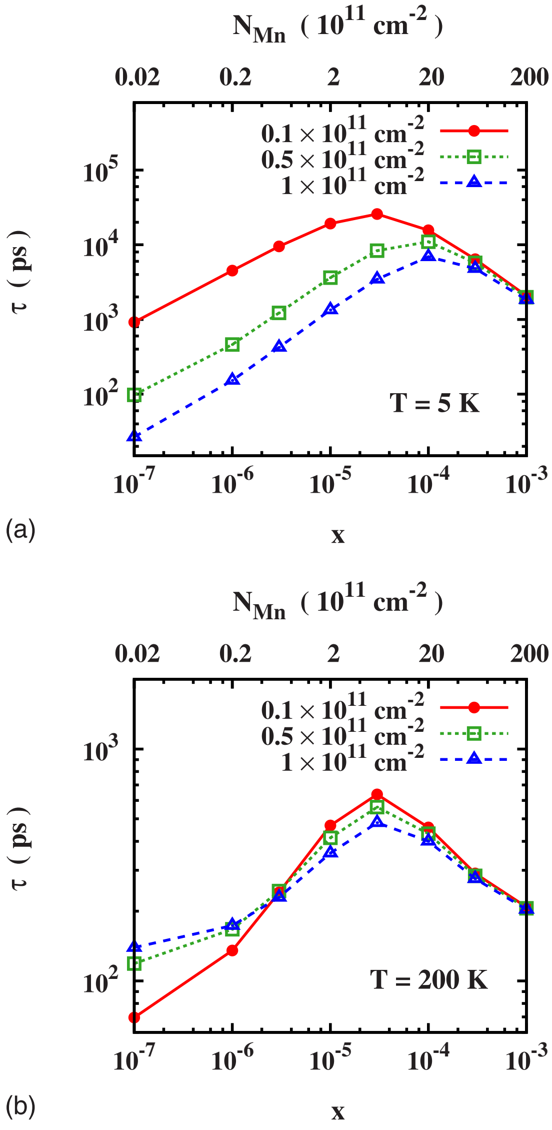

FIG. 7. (Color online) SRT τ as function of the Mn concentration for different photoexcitation densities at (a) $T=5$ and (b) 200 K. Red solid curve with ●: $N_{ex}=0.1\times10^{11}$ cm^{-2}; green dotted curve with □: $N_{ex}=0.5\times10^{11}$ cm^{-2}; blue dashed curve with △: $N_{ex}=1\times10^{11}$ cm^{-2}.

3. Photoexcitation density dependence of the SRT

We now study the photoexcitation density N_{ex} dependence of the spin relaxation. In Fig. 7 the SRT is plotted against the

Mn concentration x for three photoexcitation densities at low (5 K) and high (200 K) temperatures. It is noted that the SRT exhibits very different photoexcitation density dependences at low and high temperatures. Moreover, the photoexcitation density dependence varies with x. Let us divide the variation of x into three regimes: the small $x(x<3\times10^{-6})$ regime where the DP mechanism is dominant; the medium $x(3\times10^{-6}<x<10^{-4})$ regime where the DP mechanism is comparable with the other mechanisms; the large $x(x>10^{-4})$ regime where the DP mechanism is irrelevant.

In small x regime, the DP mechanism dominates the spin relaxation. The photoexcitation dependence of the DP spin relaxation is different in the degenerate and nondegenerate regimes. Similar to the case of n-type Ga(Mn)As quantum wells (see Sec. III A), in degenerate (low temperature) regime, the density dependence of the SRT is dominated by the increase in the inhomogeneous broadening with increasing density, and hence the SRT decreases with increasing density. In nondegenerate (high temperature) regime, the density dependence of the SRT is dominated by the increase of the electron-electron and electron-hole Coulomb scatterings with density, and hence the SRT increases.

In the large x regime, the spin relaxation is mainly due to the EY, BAP, and s-d exchange scattering mechanisms. At low temperature, the s-d exchange scattering mechanism is dominant. As $\tau_{\rm sd}$ is independent of the electron density, the photoexcitation density dependence of the SRT (which mainly comes from the EY mechanism) is weak. At high temperature, the BAP mechanism dominates. As holes are mainly from the Mn dopants and the electron system is nondegenerate, the SRT also changes little with photoexcitation density.

In the medium x regime, all the four mechanisms contribute to the spin relaxation. As $\tau_{\rm sd}$ is independent of the electron density, the density dependence comes from the other three mechanisms. At low temperature, besides the DP mechanism, the BAP mechanism is also important. However, the BAP spin relaxation changes slowly with electron (hole) density as the Pauli blocking is important at low temperature (see Fig. 4). The spin relaxation due to the EY mechanism also increases with increasing $N_{\rm ex}$ as the spin-flip matrices $[\hat{\Lambda}^{(1)}_{\mathbf{k}',\mathbf{k}}$ and $\hat{\Lambda}^{(2)}_{\mathbf{k}',\mathbf{k}}]$ in Eq. (7) increase with increasing k. However, the EY mechanism is usually less efficient than the DP mechanism for $x<10^{-4}$. As the DP spin relaxation increases with increasing photoexcitation density while other relevant mechanisms change slowly or less important than it, the peak moves to larger x with increasing photoexcitation density as indicated in Fig. 7(a). Moreover, the total SRT decreases with increasing photoexcitation density. At high temperature, as the electron system is nondegenerate, the inhomogeneous broadening changes slowly with $N_{\rm ex}$. However, the screening increases with increasing $N_{\rm ex}$ as the carrier density increases. Hence the momentum scattering (mainly from the electron-impurity scattering) decreases with increasing $N_{\rm ex}$. Therefore, the SRT due to the DP mechanism decreases with increasing $N_{\rm ex}$. The EY mechanism is less important than the DP mechanism in this regime [see Fig. 3(c)]. Moreover, as the hole system is nondegenerate, the spin relaxation due to the BAP mechanism increases with hole density. Therefore, the SRT also decreases with increasing photoexcitation density.

4. Effect of magnetic field on the SRT

We now study the effect of magnetic field on the SRT. The magnetic field is applied parallel to the quantum-well plane, which is perpendicular to the initial electron spin polarization (the Voigt configuration). In traditional nonmagnetic n-type quantum wells, where the electron spin relaxation is dominated by the DP mechanism, the magnetic field in the Voigt configuration has dual effects on spin relaxation: (i) elongating the spin lifetime by a factor of $[1+(\omega_L\tau_p)^2]$ (ω_L is the Larmor frequency, τ_p is the momentum scattering time);[26] (ii) mixing the in-plane and out-of-plane spin relaxations,[35,65] e.g., $\frac{1}{\tau}=\frac{1}{2}(\frac{1}{\tau_z}+\frac{1}{\tau_\|})$ when $\omega_L>\frac{1}{2}(\frac{1}{\tau_z}-\frac{1}{\tau_\|})$.[65] Usually, effect (i) is weak, but effect (ii) is more important. Differing from the case of nonmagnetic n-type quantum wells, there are several new scenarios in the p-type Ga(Mn)As quantum wells: (i) the magnetic field can polarize the Mn spins, which alters the spin relaxation due to the s-d exchange scattering mechanism. (ii) The nonequilibrium Mn spin polarization can be induced during the evolution through the $s(p)$-d exchange interaction with both electrons and holes. It precesses around the magnetic field and produces the Mn beats. This has been studied both experimentally and theoretically in II-VI magnetically doped quantum wells.[66,67] However, we find that the induced nonequilibrium Mn spin polarization is rather small (much smaller than the electron spin polarization) and affects the spin dynamics marginally. This is consistent with the fact that the Mn beats are not observed in p-type Ga(Mn)As quantum wells.[22] (iii) The spin relaxation due to the EY mechanism is also anisotropic because the out-of-plane spin relaxation comes from $\hat{\Lambda}^{(1)}_{\mathbf{k}',\mathbf{k}}$ while the in-plane relaxation from $\hat{\Lambda}^{(2)}_{\mathbf{k}',\mathbf{k}}$ [see Eq. (7)]. At large x when the EY mechanism is important, this anisotropy may show up.

In Fig. 8, we plot the SRT as function of the magnetic field with different Mn concentration at $T=5$ and 200 K. For the case of small $x(x=10^{-6})$, it is seen that the SRT increases abruptly when the magnetic field varies from 0 to 0.2 T and is almost a constant for $B=0.2$ to 6 T. This abrupt increase in the SRT originates from the mixing of the out-of-plane and in-plane electron spin relaxations in the presence of magnetic field. For small x, the spin relaxation is dominated by the DP mechanism. For the DP spin relaxation, the in-plane spin relaxation is slower than the out-of-plane one, as only part of the inhomogeneous spin-orbit field $\mathbf{h}(\mathbf{k})$ contributes to the in-plane spin relaxation. After the magnetic field is applied, the spin relaxation rate becomes $\frac{1}{\tau}=\frac{1}{2}(\frac{1}{\tau_z}+\frac{1}{\tau_\|})$. The condition for this relation is $\omega_L>\frac{1}{2}(\frac{1}{\tau_z}-\frac{1}{\tau_\|})$. In the situation considered here, it is $B\gtrsim0.005$ T(0.02 T) for low (high) temperature case. Therefore, the variation in the SRT with the magnetic field seems abruptly.

For the case of large $x(x=10^{-3})$, the relevant spin relaxation mechanisms at high temperature are the BAP, EY, and s-d exchange mechanisms. The BAP and s-d exchange mechanisms are isotropic. However, the EY mechanism is anisotropic. Our calculation indicates that the $\hat{\Lambda}^{(1)}_{\mathbf{k}',\mathbf{k}}$ term is smaller than the $\hat{\Lambda}^{(2)}_{\mathbf{k}',\mathbf{k}}$ term in Eq. (7). Hence the in-plane EY spin relaxation is faster than the out-of-plane one. Therefore the SRT decreases with increasing magnetic field abruptly by a small amount at low magnetic field. After the abrupt decrease, the SRT changes little with the magnetic field as the BAP mechanism is almost independent of the magnetic field. At low temperature, the dominant spin relaxation mechanism is the *s-d* exchange scattering mechanism which is isotropic. Moreover, the contribution of the EY mechanism is even smaller compared to the high-temperature case [see Figs. 3(a) and 3(c)]. Therefore, the magnitude of the abrupt decrease in the SRT at low magnetic field is even smaller than the high-temperature case. Let us now turn to the magnetic field dependence of the *s-d* exchange scattering mechanism. We choose the eigenstates of σ_x (denoted as $|\pm\rangle$) as the basis [hence $\langle s_z\rangle = -\Sigma_{\mathbf{k}} \mathrm{Im}\, \rho_{\mathbf{k}}$]. By keeping only the diagonal element of the Mn spin density matrix $\hat{\rho}_{\rm Mn}$, from Eq. (5) we obtain

$$\partial_t \sum_{\mathbf{k}} \rho_{\mathbf{k}}\Big|^{\rm scat}_{\rm sd} = -N_{\rm Mn}\alpha^2 I_s \sum_{\mathbf{k}} \rho_{\mathbf{k}} \Bigg\{ \frac{m^*}{4} S(S+1) + \langle S_x^2 \rangle - \sum_{\mathbf{k}'} \pi \delta(\varepsilon_{\mathbf{k}'} - \varepsilon_{\mathbf{k}}) \langle S_x \rangle (f_{\mathbf{k}'+} - f_{\mathbf{k}'-}) \Bigg\}. \quad (8)$$

As $(f_{\mathbf{k}'+} - f_{\mathbf{k}'-})$ corresponds to the electron spin polarization along the *x* axis which is much smaller than the Mn spin polarization as both the spin and the *g* factor of the Mn ions are larger than those of electrons. Therefore, the second term in the right-hand side of the above equation is much smaller than the first one. The spin relaxation due to the *s-d* exchange scattering mechanism increases with increasing magnetic field as $\langle S_x^2 \rangle$ does. Consequently, after the abrupt decrease in the SRT at low magnetic field, the SRT further decreases with increasing magnetic field due to the enhancement of the *s-d* exchange scattering.

We now turn to the medium *x* case ($x = 10^{-4}$). At low temperature, all the mechanisms are relevant [see Fig. 3(a)]. As the BAP and *s-d* exchange scattering mechanisms are isotropic, the anisotropy mainly comes from the DP and EY mechanisms. However, as the EY mechanism is less efficient than the DP mechanism, the anisotropy mainly comes from the DP one. Consequently, the SRT first increases abruptly due to the mixing of the in-plane and out-of-plane DP spin relaxations, and then decreases as the *s-d* exchange scattering increases with increasing magnetic field. At high temperature, the *s-d* exchange scattering mechanism is negligible. Hence after the abrupt increase, the SRT varies little with the magnetic field.

IV. CONCLUSION

In summary, we have performed a systematic investigation on the spin relaxation in paramagnetic Ga(Mn)As quantum wells from a fully microscopic KSBE approach with all the relevant scatterings explicitly included.

For *n*-type Ga(Mn)As quantum wells, where most Mn ions take the interstitial positions,[23,24,33] we find that the spin relaxation is always dominated by the DP mechanism in the metallic regime. Interestingly, the Mn concentration dependence of the SRT is nonmonotonic and exhibits a peak. This is due to the fact that the momentum scattering and the inhomogeneous broadening have different density dependences in the nondegenerate and degenerate regimes. A similar effect was found in bulk III-V semiconductors very recently.[32] Our results also are consistent with the latest experimental finding that in the low Mn concentration regime the SRT increases with Mn concentration.[23,24]

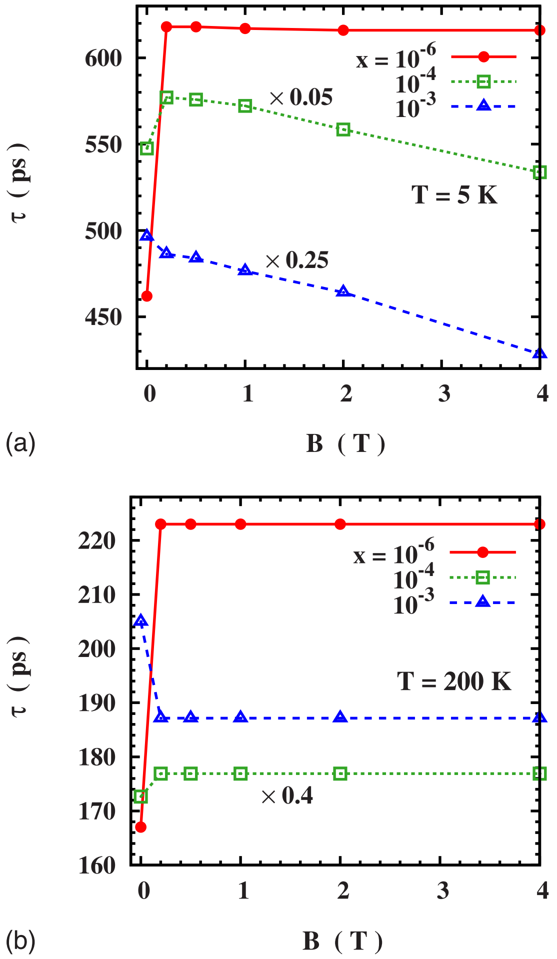

FIG. 8. (Color online) SRT τ vs the magnetic field with different Mn concentrations at (a) $T=5$ and (b) 200 K. Note that the values in the figure have been rescaled by a factor of 0.25 for the case of $x=10^{-3}$ at $T=5$ K, and 0.05 (0.4) for the case of $x=10^{-4}$ at $T=5(200)$ K.

For the *p*-type Ga(Mn)As quantum wells, we study the SRT for various Mn concentrations, temperatures, photoexcitation densities, and magnetic fields. It is found that the SRT first increases then decreases with increasing Mn concentration. The underlying physics is as follows: in the regime of small Mn concentration *x*, the spin relaxation is dominated by the DP mechanism which decreases with increasing impurity (Mn) density (hence *x*) due to motional narrowing. In the large *x* regime, as the Mn and hole densities are very large, the spin-flip scatterings such as the EY mechanism associated with the electron-impurity scattering, the *s-d* exchange scattering, and the electron-hole exchange scattering become more important than the DP spin relaxation. The SRT hence decreases with increasing Mn concentration x and the peak is formed. It is found that the most important spin relaxation mechanism at large x is the s-d exchange scattering (or the BAP) mechanism at low (or high) temperatures. The EY mechanism also contributes to the spin relaxation at intermediate temperature.

We also study the temperature dependence of the spin relaxation. The behavior also depends on the Mn concentration x as the relevant spin relaxation mechanisms are different for different x. In the small x regime, the SRT first increases then decreases with increasing temperature which resembles what was found in n-type quantum wells with low impurity density.[30] In the large x regime, at low temperature the s-d exchange scattering mechanism is dominant, which, however, is independent of the temperature. The temperature dependence is hence very weak. As the temperature increases, the EY and BAP mechanisms become more and more important, which lead to a fast decrease in the SRT with temperature. In the medium x regime, the DP mechanism is also important. As the momentum scattering is dominated by the electron-impurity scattering which changes slowly with temperature, the increase in the inhomogeneous broadening leads to the decrease in the SRT. The SRT due to the BAP and EY mechanisms also decreases with increasing temperature. Consequently, the SRT also decreases monotonically with increasing temperature in the medium x regime.

We then address the photoexcitation density dependence of the SRT. The behavior is different for different temperature and x. At low temperature, as the electron system is in the degenerate regime, the DP mechanism is largely enhanced as the inhomogenous broadening increases. However, the s-d exchange scattering mechanism is independent of the photoexcitation, and the BAP mechanism changes slowly with the photoexcitation density as the hole Pauli blocking is very strong. The EY mechanism is usually less efficient than the DP mechanism. Consequently, the peak in the τ-x curve moves to larger x value. The SRTs in the small and medium x regimes decrease with increasing photoexcitation density as the DP spin relaxation increases. However, the SRT at large x regime changes little as the spin relaxation is dominated by the s-d exchange scattering mechanism. The behavior is quite different at high temperature where the electron system is in the nondegenerate regime. In the small x regime, where the momentum scattering is dominated by the carrier-carrier Coulomb scattering as the impurity density is low. The SRT increases with increasing photoexcitation density as the carrier-carrier Coulomb scattering increases with increasing carrier density. In the medium x regime, where the electron-impurity scattering is dominant. As the screening increases with increasing carrier density, the electron-impurity scattering decreases with increasing photoexcitation density. Hence the SRT due to the DP mechanism decreases with increasing photoexcitation density. The EY mechanism is less important than the DP mechanism in this regime. Moreover, as the BAP mechanism becomes important, the SRT decreases with increasing photoexcitation density as the hole density increases. In the large x regime, the holes mainly come from the Mn dopants and the spin relaxation is dominated by the BAP mechanism, the SRT hence changes little with photoexcitation.

We also discuss the magnetic field dependence of the SRT. We find that the main effect at low magnetic field is the mixture of the in-plane and out-of-plane spin relaxations. The spin relaxation due to the BAP and s-d exchange scattering mechanisms is isotropic, whereas that due to the DP and EY mechanism is anisotropic. For the DP mechanism the in-plane spin relaxation is slower than the out-of-plane one, whereas for the EY mechanism, the in-plane one is faster than the out-of-plane one. Therefore, in small and medium x regimes where the DP mechanism is more important than the EY mechanism, the magnetic field induces an abrupt increase in the SRT due to the mixing of the in-plane and out-of-plane spin relaxations.[65] In large x regime, the EY mechanism is more important than the DP mechanism, and the SRT hence decreases abruptly with increasing magnetic field. Another important effect of the magnetic field is that it induces an equilibrium Mn spin polarization and thus enhances the s-d exchange scattering mechanism. Consequently, for large x at low temperature, where the s-d exchange scattering dominates the spin relaxation, the SRT decreases with increasing magnetic field. In other regimes, the s-d exchange scattering mechanism is unimportant and the magnetic field dependence of the SRT after the abrupt jump is also weak. We find that the nonequilibrium spin polarization transferred from the electron system to the Mn system due to the s-d exchange interaction is much smaller than the electron spin polarization, which is consistent with the fact that the Mn beats are not observed in experiments.[22]

ACKNOWLEDGMENTS

This work was supported by the National Natural Science Foundation of China under Grant No. 10725417, the National Basic Research Program of China under Grant No. 2006CB922005, and the Knowledge Innovation Project of the Chinese Academy of Sciences, the Robert-Bosch Stiftung, as well as by the DFG via Projects No. SFB 689 and No. SPP 1285.

---

*Author to whom correspondence should be addressed: mwwu@ustc.edu.cn

[1] H. Munekata, H. Ohno, S. von Molnár, A. Segmüller, L. L. Chang, and L. Esaki, Phys. Rev. Lett. **63**, 1849 (1989).

[2] H. Ohno, H. Munekata, T. Penney, S. von Molnár, and L. L. Chang, Phys. Rev. Lett. **68**, 2664 (1992).

[3] H. Munekata, A. Zaslavsky, P. Fumagalli, and R. J. Gambino, Appl. Phys. Lett. **63**, 2929 (1993).

[4] H. Ohno, A. Shen, F. Matsukura, A. Oiwa, A. Endo, S. Katsumoto, and Y. Iye, Appl. Phys. Lett. **69**, 363 (1996).

[5] T. Hayashi, M. Tanaka, K. Seto, T. Nishinaga, and K. Ando, Appl. Phys. Lett. **71**, 1825 (1997).

[6] A. Van Esch, L. Van Bockstal, J. De Boeck, G. Verbanck, A. S. van Steenbergen, P. J. Wellmann, B. Grietens, R. Bogaerts, F. Herlach, and G. Borghs, Phys. Rev. B **56**, 13103 (1997).

[7] H. Ohno, Science **281**, 951 (1998).

[8] T. Jungwirth, J. Sinova, J. Mašek, J. Kučera, and A. H. MacDonald, Rev. Mod. Phys. **78**, 809 (2006).

[9] *Diluted Magnetic Semiconductors*, edited by J. K. Furdyna and J. Kossut, Semiconductor and Semimetals Vol. 25 (Academic, New York, 1988); *Diluted Magnetic Semiconductors*, edited by M. Balkanski and M. Averous (Plenum, New York, 1991).

[10] *Semiconductor Spintronics and Quantum Computation*, edited by D. D. Awschalom, D. Loss, and N. Samarth (Springer-Verlag, Berlin, 2002); I. Žutić, J. Fabian, and S. Das Sarma, Rev. Mod. Phys. **76**, 323 (2004); J. Fabian, A. Matos-Abiague, C. Ertler, P. Stano, and I. Žutić, Acta Phys. Slov. **57**, 565 (2007); *Spin Physics in Semiconductors*, edited by M. I. D'yakonov (Springer, Berlin, 2008), and references therein.

[11] S. A. Wolf, D. D. Awschalom, R. A. Buhrman, J. M. Daughton, S. von Molnár, M. L. Roukes, A. Y. Chtchelkanova, and D. M. Treger, Science **294**, 1488 (2001).

[12] T. Dietl, in *Modern Aspects of Spin Physics*, edited by J. Fabian (Springer, Berlin, 2007), Vol. 712, pp. 1–46.

[13] C. Ertler and J. Fabian, Phys. Rev. Lett. **101**, 077202 (2008).

[14] F. Maccherozzi, M. Sperl, G. Panaccione, J. Minár, S. Polesya, H. Ebert, U. Wurstbauer, M. Hochstrasser, G. Rossi, G. Woltersdorf, W. Wegscheider, and C. H. Back, Phys. Rev. Lett. **101**, 267201 (2008).

[15] K. Wagner, D. Neumaier, M. Reinwald, W. Wegscheider, and D. Weiss, Phys. Rev. Lett. **97**, 056803 (2006).

[16] D. Saha, L. Siddiqui, P. Bhattacharya, S. Datta, D. Basu, and M. Holub, Phys. Rev. Lett. **100**, 196603 (2008).

[17] For recent advancement in spin injection from ferromagnetic semiconductors, see, M. Ciorga, A. Einwanger, U. Wurstbauer, D. Schuh, W. Wegscheider, and D. Weiss, arXiv:0809.1736 (unpublished).

[18] C. Rüster, T. Borzenko, C. Gould, G. Schmidt, L. W. Molenkamp, X. Liu, T. J. Wojtowicz, J. K. Furdyna, Z. G. Yu, and M. E. Flatté, Phys. Rev. Lett. **91**, 216602 (2003).

[19] H. X. Tang, R. K. Kawakami, D. D. Awschalom, and M. L. Roukes, Phys. Rev. Lett. **90**, 107201 (2003).

[20] H. Ohno, D. Chiba, F. Matsukura, T. Omiya, E. Abe, T. Dietl, Y. Ohno, and K. Ohtani, Nature (London) **408**, 944 (2000).

[21] J. Fernández-Rossier, C. Piermarocchi, P. Chen, A. H. MacDonald, and L. J. Sham, Phys. Rev. Lett. **93**, 127201 (2004); J. Wang, C. Sun, J. Kono, A. Oiwa, H. Munekata, L. Cywinski, and L. J. Sham, *ibid.* **95**, 167401 (2005); J. Wang, I. Cotoros, K. M. Dani, X. Liu, J. K. Furdyna, and D. S. Chemla, *ibid.* **98**, 217401 (2007); Y. Hashimoto, S. Kobayashi, and H. Munekata, *ibid.* **100**, 067202 (2008); J. Wang, I. Cotoros, X. Liu, J. Chovan, J. K. Furdyna, I. E. Perakis, and D. S. Chemla, arXiv:0804.3456 (unpublished).

[22] M. Poggio, R. C. Myers, N. P. Stern, A. C. Gossard, and D. D. Awschalom, Phys. Rev. B **72**, 235313 (2005).

[23] R. Schulz, T. Korn, D. Stich, U. Wurstbauser, D. Schuh, W. Wegscheider, and C. Schüller, Physica E **40**, 2163 (2008).

[24] T. Korn, R. Schulz, S. Fehringer, U. Wurstbauer, D. Schuh, W. Wegscheider, M. W. Wu, and C. Schüller, arXiv:0809.3654 (unpublished).

[25] K. S. Burch, D. D. Awschalom, and D. N. Basov, J. Magn. Magn. Mater. **320**, 3207 (2008).

[26] F. Meier and B. P. Zakharchenya, *Optical Orientation* (North-Holland, Amsterdam, 1984).

[27] M. I. D'yakonov and V. I. Perel', Zh. Eksp. Teor. Fiz. **60**, 1954 (1971) [Sov. Phys. JETP **33**, 1053 (1971)]; Fiz. Tverd. Tela (Leningrad) **13**, 3581 (1971) [Sov. Phys. Solid State **13**, 3023 (1972)].

[28] G. L. Bir, A. G. Aronov, and G. E. Pikus, Zh. Eksp. Teor. Fiz. **69**, 1382 (1975) [Sov. Phys. JETP **42**, 705 (1976)].

[29] Y. Yafet, Phys. Rev. **85**, 478 (1952); R. J. Elliott, *ibid.* **96**, 266 (1954).

[30] J. Zhou, J. L. Cheng, and M. W. Wu, Phys. Rev. B **75**, 045305 (2007).

[31] J. Zhou and M. W. Wu, Phys. Rev. B **77**, 075318 (2008).

[32] J. H. Jiang and M. W. Wu, Phys. Rev. B **79**, 125206 (2009).

[33] K. W. Edmonds, P. Bogusławski, K. Y. Wang, R. P. Campion, S. N. Novikov, N. R. S. Farley, B. L. Gallagher, C. T. Foxon, M. Sawicki, T. Dietl, M. Buongiorno Nardelli, and J. Bernholc, Phys. Rev. Lett. **92**, 037201 (2004).

[34] M. W. Wu and C. Z. Ning, Eur. Phys. J. B **18**, 373 (2000); M. W. Wu and H. Metiu, Phys. Rev. B **61**, 2945 (2000); M. W. Wu, J. Phys. Soc. Jpn. **70**, 2195 (2001).

[35] M. Q. Weng and M. W. Wu, Phys. Rev. B **68**, 075312 (2003).

[36] M. Q. Weng, M. W. Wu, and L. Jiang, Phys. Rev. B **69**, 245320 (2004).

[37] M. Q. Weng and M. W. Wu, Phys. Rev. B **70**, 195318 (2004).

[38] C. Lü, J. L. Cheng, and M. W. Wu, Phys. Rev. B **73**, 125314 (2006).

[39] P. Zhang, J. Zhou, and M. W. Wu, Phys. Rev. B **77**, 235323 (2008).

[40] J. H. Jiang, M. W. Wu, and Y. Zhou, Phys. Rev. B **78**, 125309 (2008).

[41] X. Z. Ruan, H. H. Luo, Y. Ji, Z. Y. Xu, and V. Umansky, Phys. Rev. B **77**, 193307 (2008).

[42] L. H. Teng, P. Zhang, T. S. Lai, and M. W. Wu, Europhys. Lett. **84**, 27006 (2008).

[43] D. Stich, J. Zhou, T. Korn, R. Schulz, D. Schuh, W. Wegscheider, M. W. Wu, and C. Schüller, Phys. Rev. Lett. **98**, 176401 (2007); Phys. Rev. B **76**, 205301 (2007).

[44] T. Korn, D. Stich, R. Schulz, D. Schuh, W. Wegscheider, and C. Schüller, Adv. Solid State Phys. **48**, 143 (2009).

[45] L. Jiang and M. W. Wu, Phys. Rev. B **72**, 033311 (2005).

[46] D. Stich, J. H. Jiang, T. Korn, R. Schulz, D. Schuh, W. Wegscheider, M. W. Wu, and C. Schüller, Phys. Rev. B **76**, 073309 (2007).

[47] A. W. Holleitner, V. Sih, R. C. Myers, A. C. Gossard, and D. D. Awschalom, New J. Phys. **9**, 342 (2007).

[48] F. Zhang, H. Z. Zheng, Y. Ji, J. Liu, and G. R. Li, Europhys. Lett. **83**, 47006 (2008).

[49] F. Zhang, H. Z. Zheng, Y. Ji, J. Liu, and G. R. Li, Europhys. Lett. **83**, 47007 (2008).

[50] E. T. Yu, J. O. McCaldin, and T. C. McGill, Solid State Phys. **46**, 1 (1992).

[51] H. Haug and A.-P. Jauho, *Quantum Kinetics in Transport and Optics of Semiconductors* (Springer, Berlin, 1998).

[52] G. Dresselhaus, Phys. Rev. **100**, 580 (1955).

[53] Y. A. Bychkov and E. I. Rashba, J. Phys. C **17**, 6039 (1984); JETP Lett. **39**, 78 (1984).

[54] W. H. Lau and M. E. Flatte, Phys. Rev. B **72**, 161311(R) (2005).

[55] R. C. Myers, M. H. Mikkelsen, J.-M. Tang, A. C. Gossard, M. E. Flatté, and D. D. Awschalom, Nature Mater. **7**, 203 (2008).

[56] *Semiconductors*, Landolt-Bornstein, New Series, edited by O. Madelung (Springer, Berlin, 1987) Vol. 17a.

[57] W. Ekardt, K. Lösch, and D. Bimberg, Phys. Rev. B **20**, 3303 (1979).

[58] M. Z. Maialle, Phys. Rev. B **54**, 1967 (1996).

[59] S. Sanvito, P. Ordejón, and N. A. Hill, Phys. Rev. B **63**, 165206 (2001).

[60] W. J. H. Leyland, G. H. John, R. T. Harley, M. M. Glazov, EL. Ivchenko, D. A. Ritchie, I. Farrer, A. J. Shields, and M. Henini, Phys. Rev. B **75**, 165309 (2007).

[61] G. F. Giulianni and G. Vignale, *Quantum Theory of the Electron Liquid* (Cambridge University Press, Cambridge, England, 2005).

[62] M. Syperek, D. R. Yakovlev, A. Greilich, J. Misiewicz, M. Bayer, D. Reuter, and A. D. Wieck, Phys. Rev. Lett. **99**, 187401 (2007).

[63] G. V. Astakhov, R. I. Dzhioev, K. V. Kavokin, V. L. Korenev, M. V. Lazarev, M. N. Tkachuk, Yu. G. Kusrayev, T. Kiessling, W. Ossau, and L. W. Molenkamp, Phys. Rev. Lett. **101**, 076602 (2008).

[64] C. Śliwa and T. Dietl, Phys. Rev. B **78**, 165205 (2008).

[65] S. Döhrmann, D. Hägele, J. Rudolph, M. Bichler, D. Schuh, and M. Oestreich, Phys. Rev. Lett. **93**, 147405 (2004).

[66] N. Linder and L. J. Sham, Physica E **2**, 412 (1998).

[67] S. A. Crooker, D. D. Awschalom, J. J. Baumberg, F. Flack, and N. Samarth, Phys. Rev. B **56**, 7574 (1997).